Vortex-Induced Vibration and Coincident Current Velocity Profiles for a Deepwater Drilling Riser

T. Srivilairit
Bechtel Corporation,
Houston, TX 77056
e-mail: tsrivila@bechtel.com

L. Manuel
Department of Civil, Architectural, and Environmental Engineering,
University of Texas at Austin,
Austin, TX 78712
e-mail: lmanuel@mail.utexas.edu

The objective of this study is to use full-scale field data on current velocities and riser motions to better understand the behavior of deepwater drilling risers. The data are comprised of riser accelerations and coincident current velocity profiles from the monitoring of vortex-induced vibration (VIV) of a drilling riser located at a 1000 m water depth site. Proper orthogonal decomposition (POD), an efficient numerical technique for characterizing the spatial coherence in a random field, is employed here to identify energetic current profiles. The accuracy resulting from the use of only a limited number of the most important POD modes is studied by comparing measured current velocity profiles with those reconstructed based on a reduced-order truncation. In addition to studying current velocity profiles, riser acceleration data from this deepwater drilling riser are also analyzed. In order to analyze the VIV response of this riser, in-line and cross-flow motions in different data segments are studied. Again, empirical POD procedures are employed—this time to derive energetic spatial vibration modes defining the riser motion. Importantly, these modes are identified without the need for either an analytical/computational model of the riser or any physical dimensions and material properties; instead, they are derived exclusively using the field data. Relationships between riser response and coincident current velocity profiles are investigated, especially for those data segments associated with observed lock-in response.
[DOI: 10.1115/1.3058684]

1 Introduction

This study, divided into three parts, is concerned with the analysis of riser acceleration data and accompanying current velocity data obtained from a deepwater drilling riser at a site where the water depth is 1000 m. The objective is to analyze these available full-scale field measurements to improve our understanding of the VIV-related behavior of risers.

The aim in the first part, which deals with the statistical analysis of current velocity measurements, is to empirically extract significant characteristics of current velocity profiles from the data with a view to establishing simplified design current profiles for risers. In realistic environmental conditions, VIV results from both the intensity and the spatial patterns in current flows that vary over the riser length. Hence, a study of the spatial statistics of the current velocity random field and empirical derivation, using field data, of energetic velocity profiles associated with VIV occurrence can be of use in riser design. The traditional approach used to derive design current profiles involves treating current velocities at each depth independently; this can be overly conservative. At the same time, establishing full-field joint distributions of the current velocity at different depths from field data can be cumbersome due to the large amount of data involved. Proper orthogonal decomposition (POD) is an efficient numerical technique that can be employed to describe spatial coherence in a random field. POD relies on an empirical orthogonal transformation of covariance or cross-power spectral density matrices of the random field and provides insightful information because it identifies energetic spatial patterns or modes in the data; for risers, current profiles can be directly derived from an array of measurements at different depths.

The second part of this study deals with analysis of the data on riser motions. Prior to analysis of these riser response measurements, the horizontal accelerations are first resolved into in-line and cross-flow components. Again, POD procedures are employed—this time to extract energetic spatial patterns of riser acceleration (or displacement) random fields that are then related to and compared with analytically based classical riser VIV modes.

Finally, in the last part of this study, results from the first two parts are taken together to relate observed riser response with characteristics of coincident current profiles. By selecting specific events from the data, the various POD-based dominant spatial patterns in the field current profiles are related to specific contrasting types of riser response associated with VIV.

2 Proper Orthogonal Decomposition

POD is a numerical method used to empirically derive orthogonal basis functions or "modes" of a stationary random field. The method was used by Lumley [1] to study turbulence; however, its origins go back to the Karhunen–Loève procedure that was proposed independently by Karhunen [2] and Loève [3]. The method has been employed in many applications such as wind engineering to identify important spatial patterns in pressures on structures, inflow turbulence for wind turbines (see, for example, Saranyasoontorn and Manuel [4]), etc. A brief review of covariance-based POD, which can be referred to as covariance proper transformation (CPT), is presented here.

Given N weakly stationary correlated random processes, $\boldsymbol{V}(t) = \{v_1(t), v_2(t), \ldots, v_N(t)\}^T$, one can establish an $N \times N$ covariance matrix, $\mathbf{C}_{\boldsymbol{v}}$, from measurements on a spatial array of N time series, $\boldsymbol{V}(t)$,

Contributed by the Ocean Offshore and Arctic Engineering Division of ASME for publication in the JOURNAL OF OFFSHORE MECHANICS AND ARCTIC ENGINEERING. Manuscript received June 27, 2007; final manuscript received September 7, 2008; published online February 26, 2009. Assoc. Editor: Eddie H. H. Shih. Paper presented at The 26th International Conference on Offshore Mechanics and Arctic Engineering (OMAE2007), San Diego, CA, June 10–15, 2007.

$$\mathbf{C}_{\boldsymbol{v}} = \begin{bmatrix} C_{v_1v_1} & C_{v_1v_2} & \cdots & C_{v_1v_N} \\ C_{v_2v_1} & C_{v_2v_2} & \cdots & C_{v_2v_N} \\ \vdots & \vdots & \cdots & \vdots \\ C_{v_Nv_1} & C_{v_Nv_2} & \cdots & C_{v_Nv_N} \end{bmatrix}_{N\times N} \tag{1}$$

The (i,j) term in the covariance matrix in Eq. (1), i.e., $C_{v_iv_j}$, represents the sample covariance between v_i and v_j computed using all the discrete-time observations in the data set; this covariance matrix is not a function of time.

By solving an eigenvalue problem, one can diagonalize $\mathbf{C}_{\boldsymbol{v}}$ so as to obtain the matrix, $\mathbf{\Lambda}$, as follows:

$$\mathbf{\Phi}^T\boldsymbol{C}_{\boldsymbol{v}}\mathbf{\Phi} = \Lambda, \quad \boldsymbol{C}_{\boldsymbol{v}}\mathbf{\Phi} = \mathbf{\Phi}\Lambda \tag{2}$$

yielding eigenvalues, $\mathbf{\Lambda} = \text{diag}\{\lambda_1, \lambda_2, \ldots, \lambda_N\}$, arranged such that $\lambda_1 > \lambda_2 > \cdots > \lambda_N$ and associated eigenvectors, $\mathbf{\Phi} = \{\boldsymbol{\phi}_1, \boldsymbol{\phi}_2, \ldots, \boldsymbol{\phi}_N\}$.

It is then possible to rewrite the original N correlated processes, $\boldsymbol{V}(t) = \{v_1(t), v_2(t), \ldots, v_N(t)\}^T$, in terms of N uncorrelated scalar subprocesses, $\boldsymbol{Z}(t) = \{z_1(t), z_2(t), \ldots, z_N(t)\}^T$ such that

$$\boldsymbol{V}(t) = \mathbf{\Phi} \cdot \boldsymbol{Z}(t) = \sum_{j=1}^{N} \boldsymbol{\phi}_j z_j(t) \tag{3a}$$

or in discrete form, at any time, t_k, we have

$$\boldsymbol{V}(t_k) = \mathbf{\Phi} \cdot \boldsymbol{Z}(t_k) = \sum_{j=1}^{N} \boldsymbol{\phi}_j z_j(t_k) \tag{3b}$$

where $\boldsymbol{\phi}_j$ represents the jth POD mode shape corresponding to the jth scalar subprocess, $z_j(t)$. The energy associated with $z_j(t)$ is described in terms of its variance, λ_j. The individual scalar subprocesses, $z_j(t_k)$, for any discrete time, t_k, can be derived by employing the orthogonality property and by using the sampled vector, $\boldsymbol{V}(t_k)$,

$$z_j(t_k) = \boldsymbol{\phi}_j^T \boldsymbol{V}(t_k) \tag{4}$$

A reduced-order representation, $\hat{\boldsymbol{V}}(t)$, may be obtained by including only the first M POD modes and associated generalized coordinates,

$$\hat{\boldsymbol{V}}(t) = \sum_{j=1}^{M} \boldsymbol{\phi}_j z_j(t) \quad \text{where } M < N \tag{5a}$$

or in discrete form, we have

$$\hat{\boldsymbol{V}}(t_k) = \sum_{j=1}^{M} \boldsymbol{\phi}_j z_j(t_k) \quad \text{where } M < N \tag{5b}$$

We will employ POD techniques to describe both the current velocity and riser acceleration random fields in separate analyses. In one case, $\boldsymbol{V}(t)$ will represent current velocity random processes in two orthogonal directions at 20 elevations over the water depth, so that the total number of POD modes, N, is then equal to 40. In the other, $\boldsymbol{V}(t)$ will represent cross-flow riser displacement random processes at eight elevations over the riser length, so that the number of POD modes, N, is equal to 8 in that case.

It may sometimes be useful to decompose a random field in the frequency domain; the conceptual framework for POD then is similar to that in the time domain except that decomposition is done using the $N \times N$ cross-power spectral density matrix instead of the covariance matrix. Such a spectral proper transformation (SPT) can provide information at any frequency of interest instead of the energy-related insights at zero time lag possible with CPT. POD modes and eigenvalues derived then are frequency dependent (see, for example, Srivilairit [5]).

It is worth noting that POD or the derivation of empirical orthogonal functions (EOFs), as the eigenfunctions have sometimes been referred to, has been used by others to derive energetic current profiles for use in riser design. For instance, a discussion of the use of EOFs and the inverse first-order reliability method (FORM) technique to derive design current profiles has been presented by Forristall and Cooper [6] where, first, EOFs are used to reduce real current profiles to contributions from a few characteristic modes and, then, inverse FORM is employed with these modes to derive profiles associated with the target return period of interest. Jeans and Feld [7] also discussed the use of EOFs for deriving design current profiles, but in their work, the current velocities were resolved into principal and transverse components that were then analyzed separately; their EOF analyses also addressed current profiles for use in riser fatigue modeling. Meling and Eik [8] assessed the accuracy of the EOF method for simplifying the current velocity field in terms of estimates of riser fatigue damage obtained using an EOF scatter diagram.

In contrast to these other studies cited, the present study addresses the use of POD techniques for full two-dimensional current velocity profiles. The efficiency and accuracy resulting from the use of a limited number of POD modes are studied by comparing measured profiles with those based on a reduced-order POD mode truncation. Significant patterns in profiles associated with VIV occurrence are also studied using POD.

With regard to problems in structural dynamics, POD procedures can be employed to extract dominant modes of structural response directly from measurements, without the need for an analytical model or physical properties of the structure. In a related application of POD to that of the present study, Kleiven [9] demonstrated its use with model test data of a long free span pipeline response when exposed to current. Vibratory mode shapes, amplitudes, and frequencies were estimated from EOF mode shapes and generalized coordinates (time modulations). It was noted that the EOF technique may not provide appropriate information when used to decompose nonstationary response processes due to inherent limitations of the technique; importantly, though, in such cases, derived EOF modes can describe dominant features of the nonstationary response, which are different from classical vibration modes. Other applications of POD for empirically examining the dynamic response of different structures and associated derived vibratory modes exist in the literature. Aschheim et al. [10] illustrated its use on a 12-story building responding linearly and nonlinearly to earthquake ground motions; Feeny [11] demonstrated its use for obtaining information regarding the dominant states of vibration for simple structural systems.

3 Field Data

This study involves the analysis of current velocity and riser acceleration data from the monitoring of VIV of a deepwater (1000 m) riser. The data were recorded every 4 h over a 2 month period, producing more than 300 events; an "event" refers to any single such 4 h data sample. For each event, riser accelerations were recorded as 30 min time series, while the current velocity data were taken at two discrete points in time, 10 min apart. The two data sets were recorded separately and associated with a single event; the first acceleration measurement in the time series data was collected 40 min after the second of the two current velocity measurements. As a result, measured current profiles do not exactly coincide in time with the recorded riser response data. It is worth noting though that the current velocities at the site were seen to vary very slowly with time; they did not vary significantly over a duration of 4 h and varied even less over the duration of the riser motion measurements (i.e., 30 min). As such, the current velocity measurements may be reasonably assumed to describe flow conditions during the riser acceleration measurements, and the two measurements (current and riser motion) were thought to be representative for each 4 h event analyzed.

Current velocity data. These data consist of the magnitude and direction of currents at each level; every 4 h, current velocities

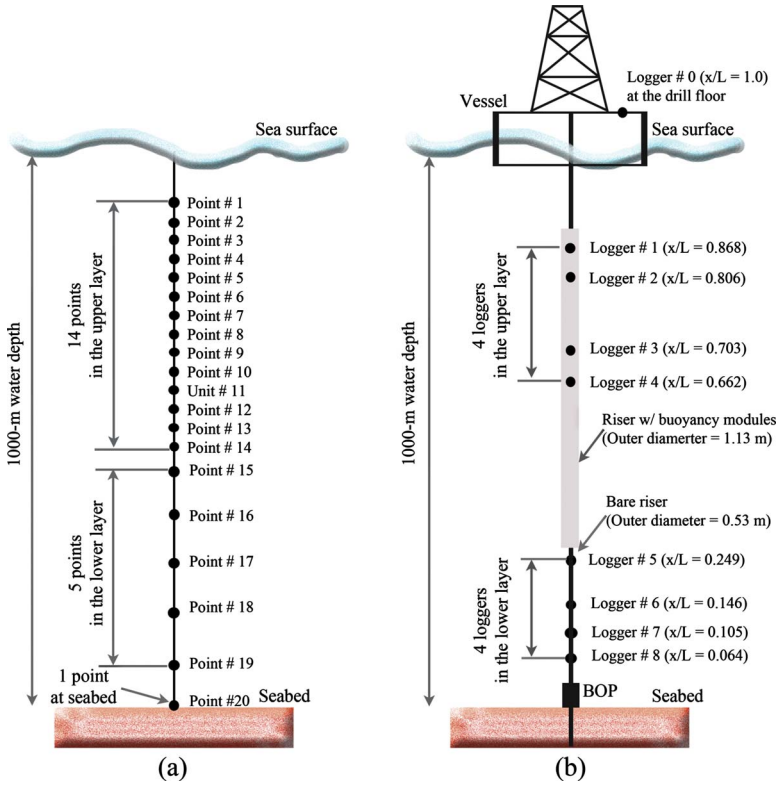

Fig. 1 Locations of (*a*) current velocity measurement units and (*b*) riser acceleration loggers

were obtained at 20 levels along the water depth using both an acoustic Doppler current profiler and one single point current meter 5 m from the seabed. The measurement locations are shown schematically in Fig. 1(*a*). Measured current velocity data, representing speed and direction, were transformed into components in two orthogonal directions (0 deg and 90 deg) at each elevation.

Riser acceleration data. These data include measurements in two horizontal (X and Y) directions and one vertical (Z) direction. Every 4 h, the data were collected for 30 min at a sampling rate of 10 Hz at eight loggers along the riser and one additional logger to measure vessel motions. Figure 1(*b*) shows a sketch of the riser with logger locations. Because the true orientations of the logger axes were unknown, a vector rotation (spectral) procedure was used to resolve the measured X and Y acceleration data into in-line (X') and cross-flow (Y') acceleration components, assuming that the dominant VIV response is transverse to the current velocity (see Srivilairit and Manuel [12]). Riser displacement time series were obtained by double integration of the rotated acceleration time series.

It is important to point out that the acceleration data available are likely contaminated by time-varying disturbance due to gravitational acceleration. This gravity contamination occurs when a logger rotates out of the vertical plane. Kaasen [13] recommended a procedure to obtain lateral motions corrected for gravity contamination, but this requires angular velocity measurements along the riser, which were not available here. As such, the riser accelerations and displacements obtained by double integration used later in the analyses may contain errors resulting from gravity contamination. It should be pointed out that field studies are, due to practical and economical considerations, generally limited in the spatial resolution of available loggers. Isherwood [14] suggested that it is only in ideal conditions, with good spatial distribution of loggers and where a single mode of vibration with constant amplitude and frequency is considered, that gravity contamination can be corrected for. When logger measurements are sparse, when the possibility of multiple modes exists, and when both amplitude and frequency vary with time, it is not as easy to perfectly correct for gravity contamination. Despite these difficulties, though, given the relative scarcity of full-scale field studies such as the one reported on here, it is worthwhile to study VIV response data from any such available studies even when data are sparse. Besides, it should also be noted that for very long risers (as is the case here), gravity contamination is expected to be smaller than has been reported in other studies such as with the 360 m riser discussed by Isherwood [14]; this is because the ratio of the maximum VIV amplitude to the maximum gravitational amplitude for single-mode VIV (SM-VIV) is directly proportional to the length of the riser.

To investigate the variation of the current velocity field data with depth, a histogram of current speed magnitudes was calculated, as shown in Fig. 2, in which darker colors represent measurements closer to the sea surface, while lighter colors represent deeper measurements. It can be seen that currents in the upper

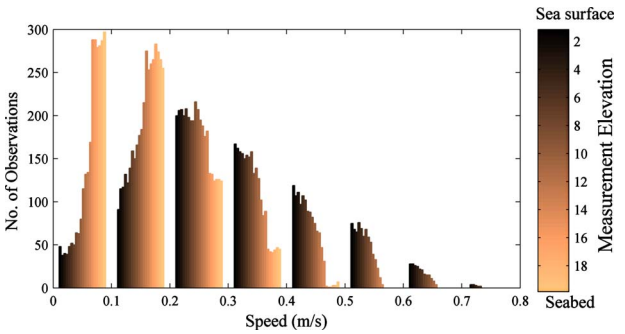

Fig. 2 Histogram of current speed magnitudes at different measurement vertical levels along the depth

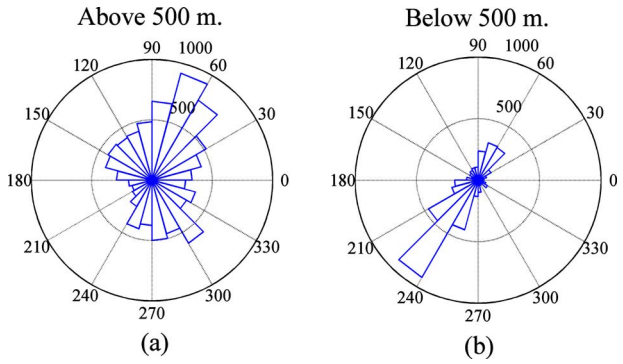

Fig. 3 Circular histograms of current directions in (*a*) the upper 500 m and (*b*) the lower 500 m

layer are strong (with maximum values at around 0.8 m/s) but exhibit great variation, whereas currents in the lower layer are weaker but more consistent (show less variability), fluctuating mostly in a small range of 0.1–0.3 m/s.

The variation of current direction with depth is also of interest. This is studied by examining circular histograms of current directions (i.e., current roses) for the upper and lower layers separately (see Fig. 3). Currents in the upper 500 m exhibit greater variability in flow direction than those in the lower 500 m, which mostly flow in one dominant direction. Also, currents at this site on average flow mainly in one vertical plane, but in opposite directions in the two layers. This average pattern by no means occurs all the time; bidirectional and orthogonal current profiles in the upper and lower halves of the water column occur often.

Note that though current velocity and riser acceleration data are not perfectly time synchronized due to the nature in which these data were recorded and though riser accelerations could be gravity contaminated, this study offers useful insights on the current velocity field separately and on relationships between the current and riser acceleration data. These insights are expected to be not greatly influenced by these data-related difficulties.

4 POD Analysis of Current Data

To estimate the extent of vertical coherence in current velocity, POD analyses of the data, representing full two-dimensional speed and direction profiles, were carried out. The current velocity components in two orthogonal directions (0 deg and 90 deg) at all 20 elevations yielded 40 random processes. The current velocity components in the 0 deg direction for the entire measurement period can be denoted by $v_1(t), v_2(t), \ldots, v_{20}(t)$, while the components in the 90 deg direction can be denoted by $v_{21}(t), v_{22}(t), \ldots, v_{40}(t)$, following the notation and general formulation for POD analysis presented in Eqs. (1)–(5). A 40×40 covariance matrix based on the current data was estimated, and a total of 40 POD modes were then derived. The first five dominant POD eigenvectors, $\boldsymbol{\phi}_j$ (hereinafter also referred to as "POD mode shapes"), obtained by arranging modes based on decreasing energy (i.e., eigenvalue), are shown in Fig. 4. The POD mode shapes, $\boldsymbol{\phi}_j$, are mutually orthogonal eigenvectors derived based on the entire current velocity data set, not on a single measured event nor on a single specified time. The eigenvalues, λ_j, associated with the energy of mode j, are indicated in terms of the percentage of the total energy in the current velocity field, which is equal to 1.46 m^2/s^2.

The mode shapes are presented in two formats: as 0 deg and 90 deg components, and as a resultant and associated direction. The first mode is predominantly in the 90 deg direction and has negligible contribution in the 0 deg (true north) direction along the water column and especially in the upper layer. In contrast, again primarily in the upper layer, the second POD mode (about half as energetic as the first mode) displays virtually no contribution in

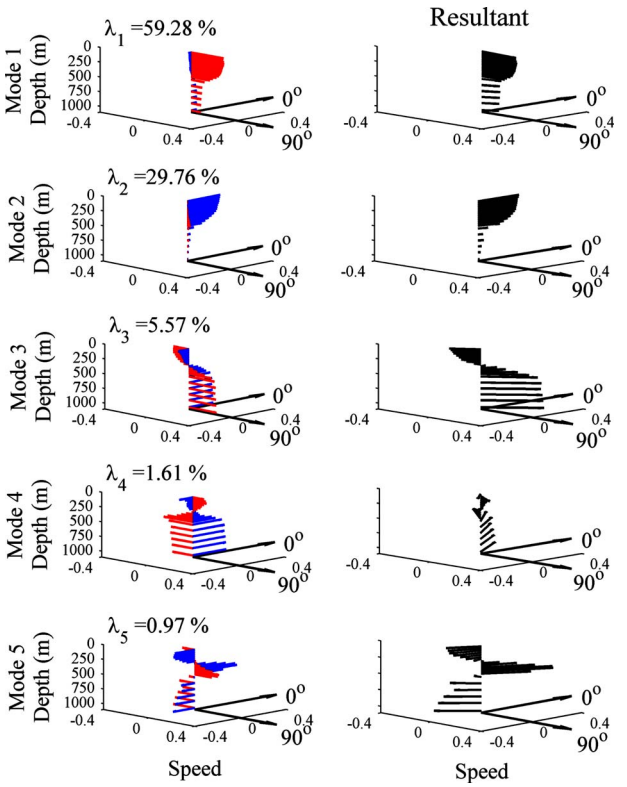

Fig. 4 First five POD modes of the current velocity for the entire data set

the 90 deg direction but relatively much larger contribution in the 0 deg direction. Mode shape resultants for the first two modes are, therefore, almost perpendicular to each other. The third POD mode (with far less energy than that in the first two modes) displays a rather sheared current profile: velocities at uppermost and lowermost depths are in nearly opposite directions. This mode has comparable amplitudes in the 0 deg and 90 deg directions; as a result, the resultant for this third mode is oriented roughly 45 deg relative to the first two modes.

While the first two POD modes together account for almost 90% of the total energy and the first mode alone almost 60%, it is useful to examine the energy distribution, by POD mode, at each elevation separately. The fraction of the variance accounted for by the POD-based reconstructed current velocity data at any level in the water column to the total variance estimated directly from measured data at that level is

$$\%\ \text{of total variance} = \frac{\text{Var}(\hat{V}_X) + \text{Var}(\hat{V}_Y)}{\text{Var}(V_X) + \text{Var}(V_Y)} \times 100\% \qquad (6)$$

where $\hat{V}_X$ and $\hat{V}_Y$ denote the reduced-order 0 deg and 90 deg current components based on a specified number of POD modes, while V_X and V_Y denote the actual measured 0 deg and 90 deg current components. In Fig. 5, it is seen that in the upper layer, the first two modes account for more than 95% of the total variance or energy in the current field. However, in the lower layer, at least four modes are needed to capture around 90% of the total variance at each depth there. In the transition zone between the upper and lower layers, more than five modes are needed to account for 90% of the total variance. For reference, Fig. 5 also shows the total current velocity variance (in $(m/s)^2$) at each level along the depth of the water column.

The current velocity field in the 0 deg and 90 deg directions based on three POD modes (i.e., computed using Eq. (5) with $M=3$) is shown in Fig. 6 for the entire 2 month period. For both

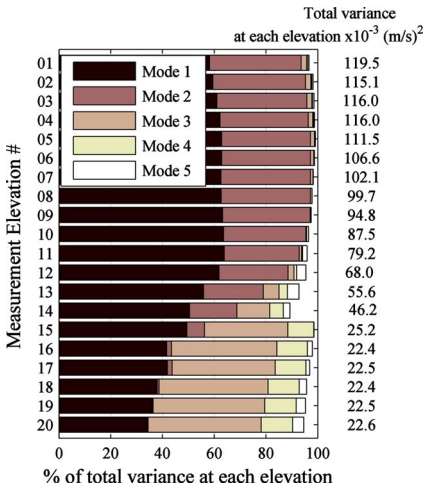

Fig. 5 Variance of the current field at different levels based on reconstruction using different numbers of POD modes

directions, plots of reconstructed current velocity can be directly compared with measured values; only in the lower layers are some differences evident.

Finally, it is of interest to investigate how efficiently the first few POD modes can capture second-moment statistics of the two-dimensional current profiles at all elevations jointly. Figure 7 presents correlation coefficients for the current data in different ways: (a) among pairs of 0 deg current velocity components (at different levels), (b) among pairs of 90 deg components, and (c) between the 0 deg and 90 deg components. Reconstructed two-dimensional current velocity profiles based on three POD modes generally preserve the observed correlation structure adequately well for all cases and at all depths; the only exception is for correlation between the 0 deg and 90 deg components where three POD modes do not predict the correct correlation; slower convergence here is due to weak correlation between 0 deg and 90 deg components. POD efficiency is greatest when correlation levels are large. Overall, though, Figs. 6 and 7 indicate that reconstructed current profiles based on three POD modes can accurately represent the statistical characteristics of the current profiles at the site studied.

5 POD Analysis of Riser Motion Data

POD procedures are employed next to empirically identify dominant spatial vibration modes or patterns of riser motion. Note that these vibration modes can be extracted from field data using POD without the need for a mathematical model of the riser. Kleiven [9] demonstrated the use of an EOF procedure, basically the same as the POD procedure, for identifying predominant vibration modes, including modal amplitudes and frequencies, from a model test of a pipeline in a long free span exposed to current.

POD is applied here to riser displacement data (obtained after, first, rotating measured accelerations into in-line and cross-flow directions and, next, carrying out double integration, as described in Srivilairit and Manuel [12]). Unlike the POD analysis of current velocity data where the POD procedures are applied to the entire measured current velocity data, in this POD analysis, riser motion data of each event (represented by a 30 min time series) are analyzed separately to extract dominant spatial patterns of riser motion for each such event. The analysis does not rely on any information on the physical properties of the riser. In principle, cross-flow and in-line displacements can be treated either separately or together; here, the cross-flow riser displacement data (of most interest) obtained at eight logger elevations over the riser length represent eight correlated stochastic processes, $\boldsymbol{V}(t) = \{v_1(t), v_2(t), \ldots, v_8(t)\}^T$, so that the maximum number of POD modes is also equal to 8. The first POD mode, $\boldsymbol{\phi}_1$, which accounts for the largest contribution of the entire riser motion's spatiotemporal field variance or energy, is expected to have a shape that closely resembles that of a dominant riser natural mode of vibration, especially for lock-in events.

Riser motions are studied by focusing on a small sample of events that represent different 30 min samples of data obtained every 4 h during the measurement campaign. In this study, power spectra for riser accelerations in two orthogonal directions (cross-

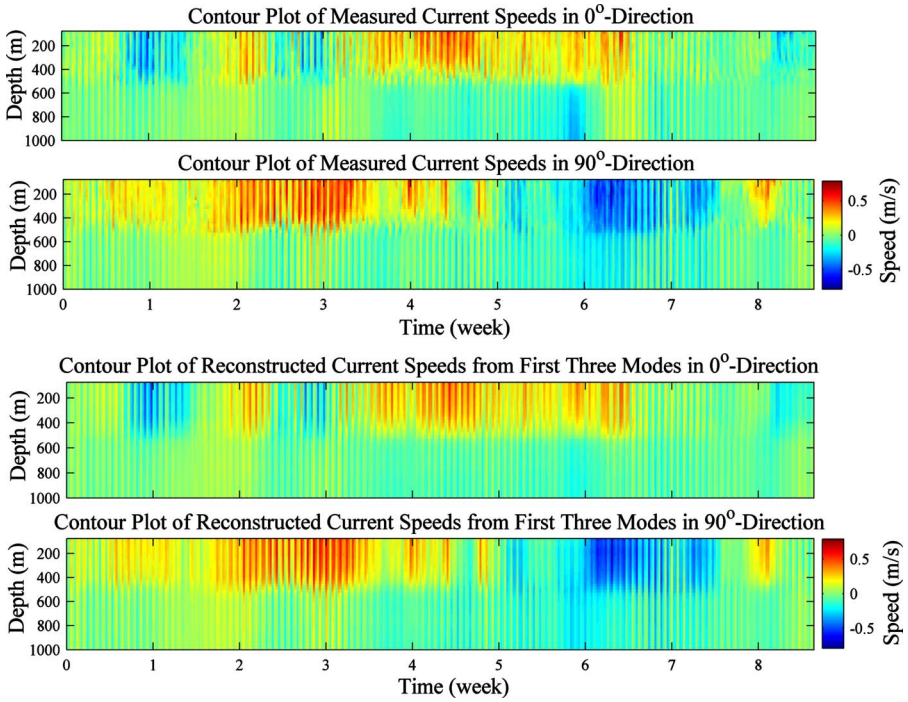

Fig. 6 Measured and reconstructed (using three POD modes) current velocity profiles over the 2 month monitoring period

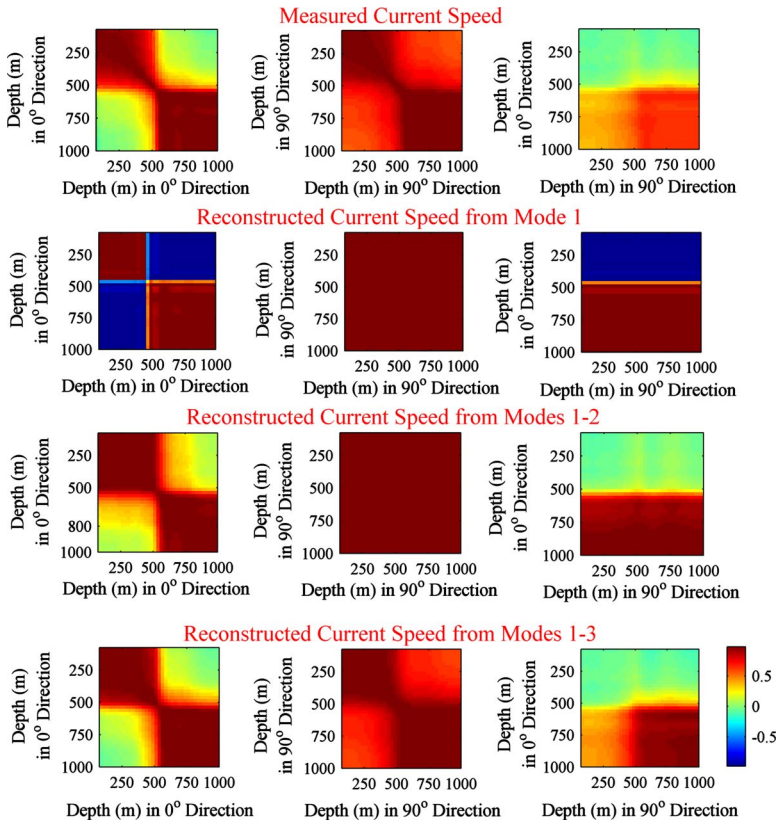

Fig. 7 Actual and POD-based correlation coefficient estimates between current components at various depths

flow and in-line) are estimated to identify whether or not VIV is indicated in each event. VIV identification is assumed to be possible by examining whether or not one or more narrow-band peaks in the power spectra are clearly indicated. A single narrow-band peak could be a possible indication of single-mode VIV (SM-VIV) response; multiple peaks could indicate multimode VIV (MM-VIV) response. The occurrence of VIV lock-in for any event can also be identified or confirmed based on the frequency-doubling phenomenon, according to which the dominant frequency in the power spectrum of the in-line acceleration is expected to occur at twice the dominant frequency in the power spectrum of cross-flow acceleration. A total of 12 events are used as illustrative examples: six single-mode VIV, three MM-VIV, and three non-VIV events. Power spectra of accelerations in cross-flow (Y') and in-line (X') directions for the 12 events at all loggers are presented in Fig. 8. For each event, relevant natural frequencies of the riser as calculated by modal analysis are also indicated. Narrow-band peaks in the cross-flow direction (Y') and frequency doubling in the orthogonal in-line direction (X') are evident for the nine VIV events and absent for the three non-VIV events. By comparing dominant peak frequencies with riser natural frequencies estimated using a riser analysis program, we can approximately identify the vibration mode associated with VIV response, especially with the single-mode VIV events. For example, SM-VIV event numbers 2, 4, and 5 have single dominant peak frequencies that roughly match the calculated natural frequency of riser modes 3, 6, and 4, respectively. Excited riser modes for SM-VIV event numbers 1, 3, and 6 are somewhat ambiguous. For the multimode VIV events, more than one spectral peak is observed; as many as three dominant frequencies are seen in the cross-flow acceleration power spectra. The 12 selected events included three non-VIV events, which expectedly exhibit neither narrow-band peaks in cross-flow response power spectra nor the frequency-doubling phenomenon.

By applying CPT-type POD analyses to the 8×8 covariance matrix estimated from the displacement data, a total of eight POD modes were derived for the cross-flow response of each of the selected events. The first three POD mode shapes for these cross-flow displacements for the 12 selected events are shown in Fig. 9. The primary POD mode shapes show some consistency in pattern among themselves and with the classical riser VIV modes associated with the dominant frequencies for each event (as were indicated in Fig. 8). For example, for the single-mode VIV events, the primary POD mode shapes of event number 1 are very similar to those of event number 2, the primary POD mode shapes of event number 3 are very similar with those of event number 4, and the primary POD mode shapes of event number 5 are very similar with those of event number 6.

Despite inadequate spatial resolution in the logger locations, Fig. 9 suggests that there is fairly good consistency of the first POD mode shape with a riser vibration mode. Differences between the dominant POD mode shape and an associated appropriate vibration mode shape in each case may be due to unaccounted for energies in higher POD modes. In addition, though, this discrepancy could be because an imprecise classical vibration mode shape is used for the riser due to assumed top tension and internal fluid mass as well as the values of structural damping used. Note that the derived empirical POD modes reflect actual preferred spatial distributions of energy in orthogonal basis functions; no assumptions on physical riser properties are required. While spectral methods alone can be used to determine which riser mode is excited in a given event (Srivilairit and Manuel [12]), with POD analyses, one can rely on the expected consistency of the first POD mode shape with potential riser modes to confirm whether or not that riser mode was indeed excited. For instance, from the plots of POD mode shape 1 along with the potential riser modes for single-mode VIV event number 1, a reasonable match is indicated between this first POD mode and the third riser vibration

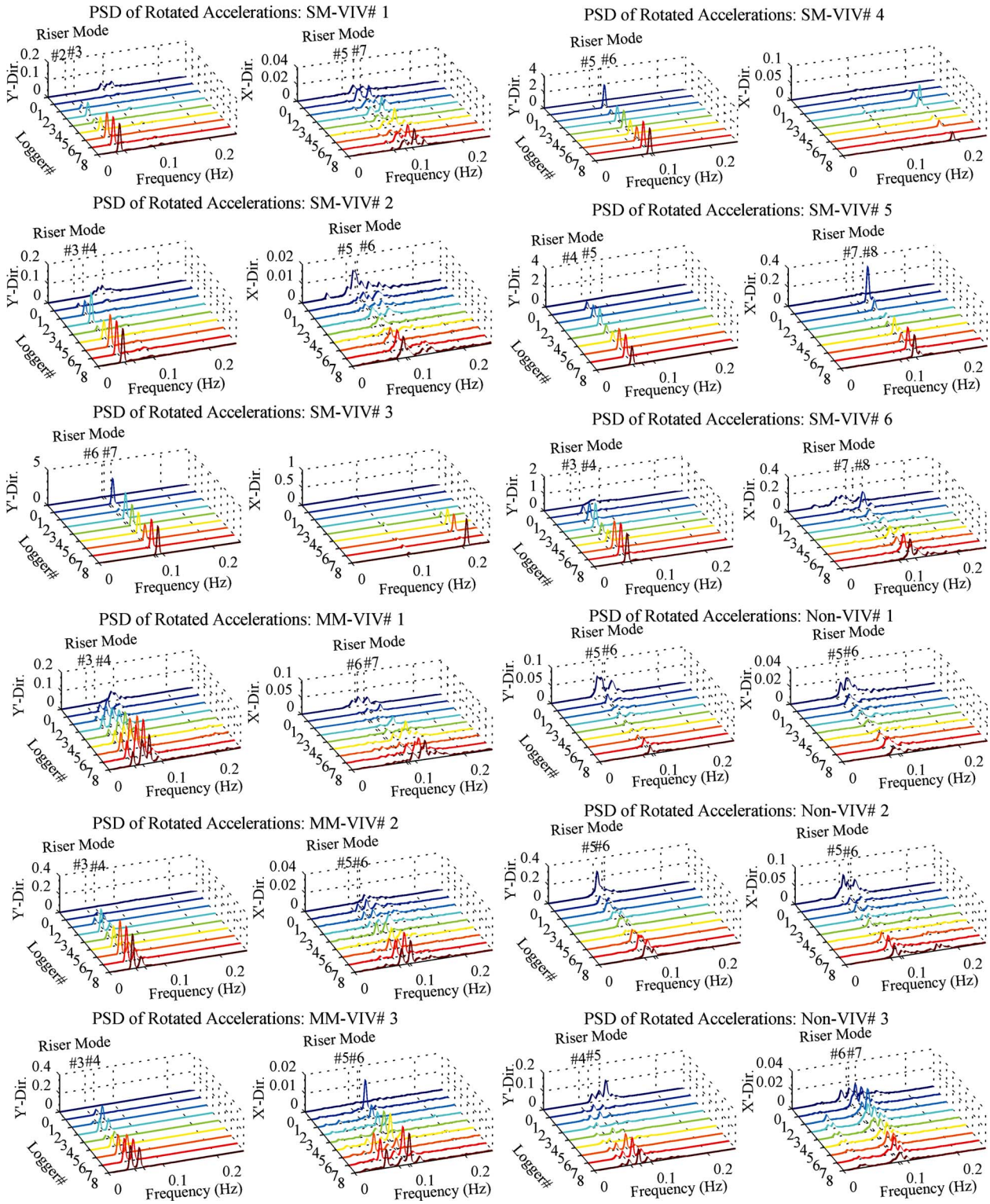

Fig. 8 Welch power spectra of rotated accelerations at nine loggers in the cross-flow (Y') and in-line (X') directions

mode. Similarly, for single-mode VIV event numbers 3 and 6, the sixth and fourth riser modes, respectively, are the matching natural vibration modes. Spectral methods alone leave some ambiguity with regard to which is the excited vibration mode (see Fig. 8) for these two events; POD helps establish, based on the spatial pattern, the riser mode most likely excited.

Note that for multimode VIV events whose power spectra show more than one spectral peak, the first POD mode shape exhibits less consistency with potential riser vibration mode shapes; higher POD modes are also not helpful in isolating the multiple riser vibration modes. For non-VIV events, expectedly, the first POD mode does not resemble any riser vibration mode; moreover, this first POD mode does not dominate the energy in riser motion, which is an indicator that lock-in is not observed.

It is important to emphasize that CPT-based POD modes might resemble relevant riser natural vibration modes in VIV events, but

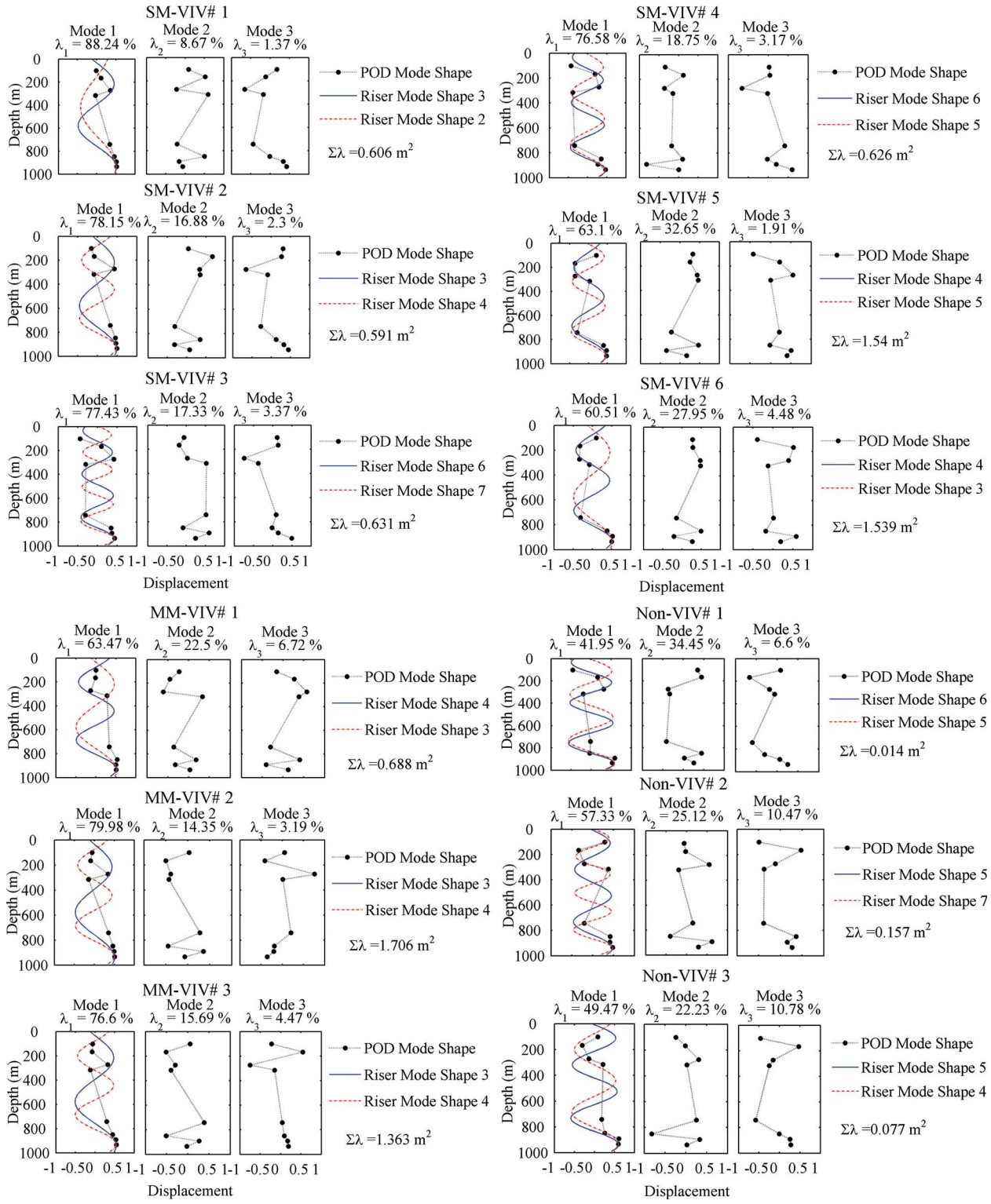

Fig. 9 The first three POD mode shapes of cross-flow riser displacements

these POD modes are extracted using an empirical procedure that requires only second-moment statistics of the data and does not rely on any spectral information. With better spatial resolution of loggers, it is conceivable that empirically derived POD mode shapes could confirm analytically predicted vibration mode shapes for a riser. The distribution of energies in these empirical shapes (the POD modes) can help to confirm separately the energy contributions from distinct peaks of power spectra in single- or multimode VIV events.

The sum of the POD eigenvalues, $\Sigma\lambda$ (or total energy) and the eigenvalue, λ_j, associated with the energy in each mode j, as a percentage of the total energy, is shown in Fig. 9. Note that large

vibration amplitudes over the length of the riser are indicated by high values of the POD eigenvalue sum, which is simply the sum of the variances of the displacements at all loggers. VIV events are distinguished from non-VIV events by the fact that the first few extracted POD modes have dominant high energy; indeed, for the nine VIV events, the first mode alone, on average, accounts for more than 70% of the entire riser motion's spatial-temporal field variance. That there is no lock-in or preferred spatial patterns in non-VIV events is evidenced by the relatively much smaller contribution from the first few POD modes there (on average only around 50% of the field energy comes from the first mode). This suggests that POD can also be used as an approximate indicator of lock-in response by examining both the proportion of the total riser motion energy derived from the first few dominant POD modes and the total energy itself.

The use of POD procedures for analyzing riser response from field data has demonstrated the ability to decompose such data into apparent vibration modes; sometimes, only a few POD mode shapes are needed to help confirm lock-in and VIV, despite the poor spatial resolution of loggers along the riser's length. Also, POD techniques can be used to determine which riser vibration mode(s) dominate the response by comparing the first POD mode shape with potential riser modes predicted, say, by a modal analysis program. Importantly, apart from the field data, no physical properties or dimensions of the riser nor any detailed analytical or computational model of the riser is needed to carry out the POD analysis and identify important vibration modes. In addition, POD methods offer a supplementary tool for detecting VIV response in riser motion measurements by considering the energy contribution of the first few dominant POD modes.

6 Riser Response and Coincident Current Profiles

The spatial patterns in current profiles corresponding to the 12 selected VIV and non-VIV events are studied next to investigate relationships between riser response and coincident current profiles. Root-mean-square (rms) riser displacements in both cross-flow and in-line directions are estimated from the doubly integrated measured riser accelerations; these are studied along with the coincident current profiles. Note that under lock-in conditions, high values of rms displacements are expected due to larger vibration amplitudes that typically accompany VIV. The current profiles associated with the 12 selected events are shown in Fig. 10. The first column of each panel in the figure shows current speed magnitude along the water column, together with rms values of the riser and vessel displacements in both cross-flow and in-line directions. The corresponding current directions, along with the direction of the peak response in the riser (indicated as angle of rotation), are shown in the second column. It should be pointed out that while the current direction is known relative to true north (expressed as °T), the relation between current and response directions is unknown due to the lack of information on the orientation of the logger axes. For convenience, however, both directions are presented together only to indicate the variation of current direction and peak response direction with depth. In the last column, the resultant current velocity profiles are presented as three-dimensional plots.

A point of clarification is appropriate here with regard to the relationship between current direction and riser cross-flow response direction. The former is identified directly from the current measurements. The latter is systematically determined by rotating the two components of riser acceleration at each logger and by studying power spectra peaks until the *maximum* of all such peaks is found; the associated direction of this peak response is then the cross-flow response direction. By definition, the current direction is transverse to this direction (Srivilairit and Manuel [12]). Dealing with complex current profiles, as is the case here with changing dominant directions over the depth, complicates riser motion description, as evident in Fig. 10; the logger orientation uncertainty for riser motions though is not a significant problem due to the rotation procedure employed.

As can be observed in Fig. 10, the riser generally experienced VIV when exposed to well-structured current profiles flowing entirely within one vertical plane. Also, it can be noticed that even low current velocities, for instance, in single-mode VIV event number 1 corresponding to riser mode 3, compared with the higher currents seen in single-mode VIV event number 3 corresponding to riser mode 6, can produce relatively large amplitudes of motion. This is likely because the proportion of the power-in region or the excitation zone in the first case is larger, and the other regions that produce hydrodynamic damping are smaller than in the second case. Besides, surprisingly large vibrations are observed in multimode VIV response, as can be seen in multimode VIV event numbers 2 and 3, for example. Generally, lower rms response is expected in multimode lock-in since wake synchronization is dramatically reduced when several modes are excited, as has been pointed out by Vandiver et al. [15]. Thus, it seems that in realistic environmental conditions where currents vary greatly with depth, VIV response can be far more complicated than in laboratory experiments.

Regarding the three non-VIV events presented in Fig. 10, three contrasting current profile patterns are seen: a low current profile with an average of roughly 0.1 m/s over the depth, a highly sheared current profile, and a bidirectional current profile. Lock-in response was rarely observed for events during which the riser was exposed to these three types of current variation over depth. It has generally been noted that lock-in response is not likely to occur when long flexible cylinders are exposed to strongly sheared flows, as is the case with non-VIV event number 2. However, Vandiver et al. [15] observed that lock-in may occur under highly sheared conditions when the power available to one particular mode can dominate that in all other modes, and this behavior has been observed in the present study as well.

7 Pod-Based Current Profiles and Different Riser Response Types

In order to represent all of the field data collected over the 2 month monitoring period, every recorded event was classified into four data sets according to the type of riser response; namely, single-mode VIV, multimode VIV, non-VIV, and "unusual" response. (Note that all events for which the riser response was greatly influenced by vessel motions were categorized as unusual response events regardless of whether lock-in occurrence was noted or not.) A total 120 single-mode VIV events, 52 multimode VIV events, 135 non-VIV events, and 33 unusual events were included. POD techniques were employed to empirically identify predominant energetic spatial profiles of the current velocity field in each data set except for the unusual data set. Using POD for all the events in each data set taken together, dominant energetic current profiles in the data set associated with single-mode VIV response of the riser are compared with profiles from the multimode VIV data set as well as those for the data set when VIV was not indicated.

The first three POD mode shapes along with associated eigenvalues, for the single-mode VIV, multimode VIV, and non-VIV data sets, are presented in Fig. 11. The mode shapes are shown in two formats: (a) as components in the 0 deg and 90 deg directions and (b) as a resultant and associated direction. Differences between each of the first three mode shapes taken separately for each of the VIV data sets are insignificant. That is, in both VIV data sets, the dominant current profiles described by the first two POD mode shapes flow almost entirely in one plane along the entire water depth with very slight shear observed. On the other hand, the first two mode shapes in the non-VIV data set suggest markedly different spatial profiles; in the first mode, the current in the upper layer flows in a direction that is nearly 45 deg separated from the direction in the lower layer, and the two layers experience fairly comparable current speeds. A highly sheared current

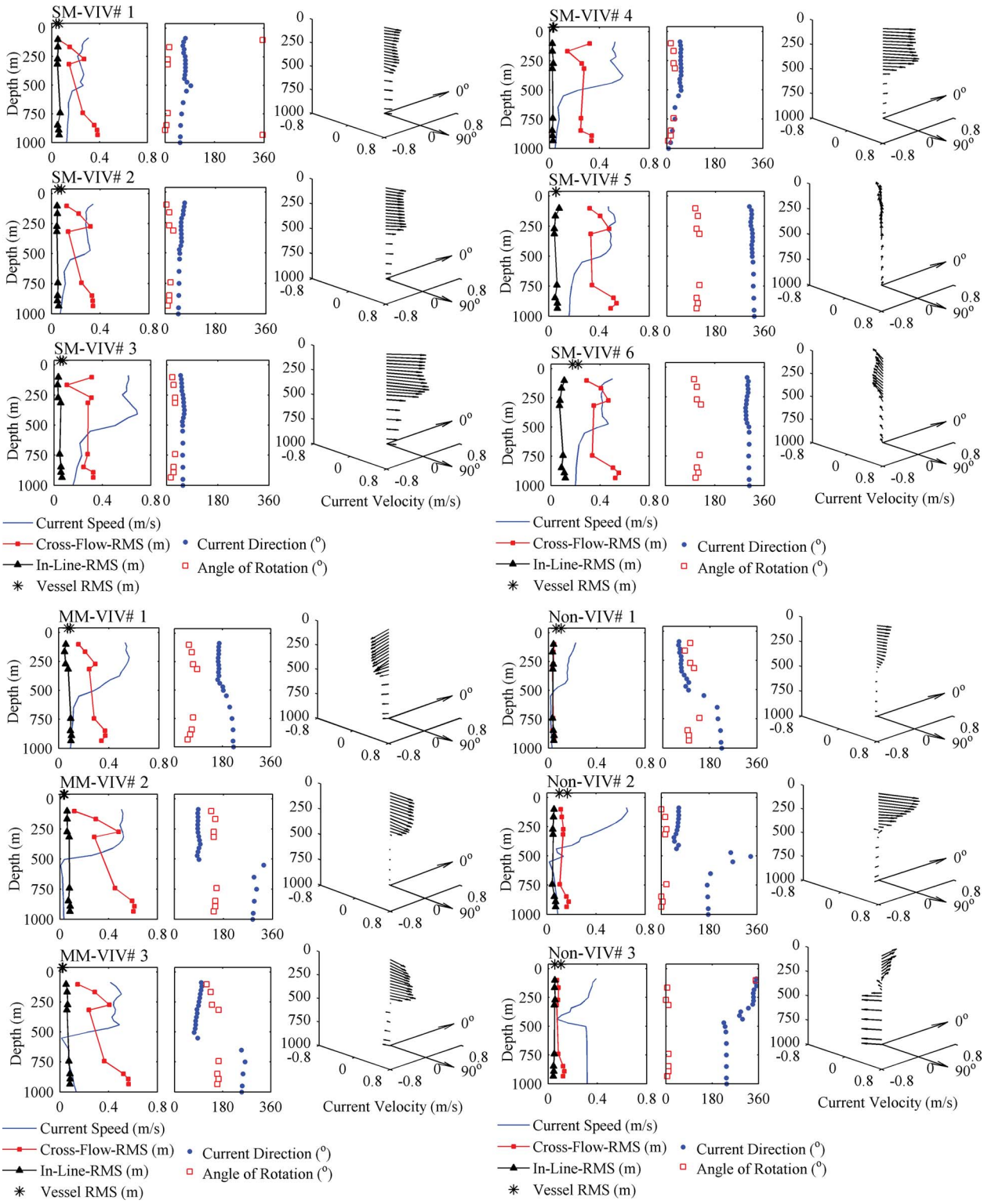

Fig. 10 Current profiles, riser and vessel rms displacements, and dominant current and riser response directions

pattern is observed in the second mode shape for this non-VIV data set. These two mode shapes show some consistency with the current profiles seen for the three selected non-VIV events discussed earlier. Note, too, that the total energy in the current velocity field, denoted by the summation of eigenvalues in Fig. 11, suggests higher energy or variance levels in both VIV data sets compared with the non-VIV data set. Additionally, the first few POD modes when they dominate—as they do for the VIV data sets—can reveal some discernible relationship between the vertical structure of the current profile and the VIV response, although the relationship between current profile patterns and the nature of VIV response (whether single mode or multimode) is less clear.

8 Conclusions

To gain an understanding of vortex-induced vibration response in a riser under realistic conditions, the analysis of full-scale field data that included both current velocities and riser accelerations

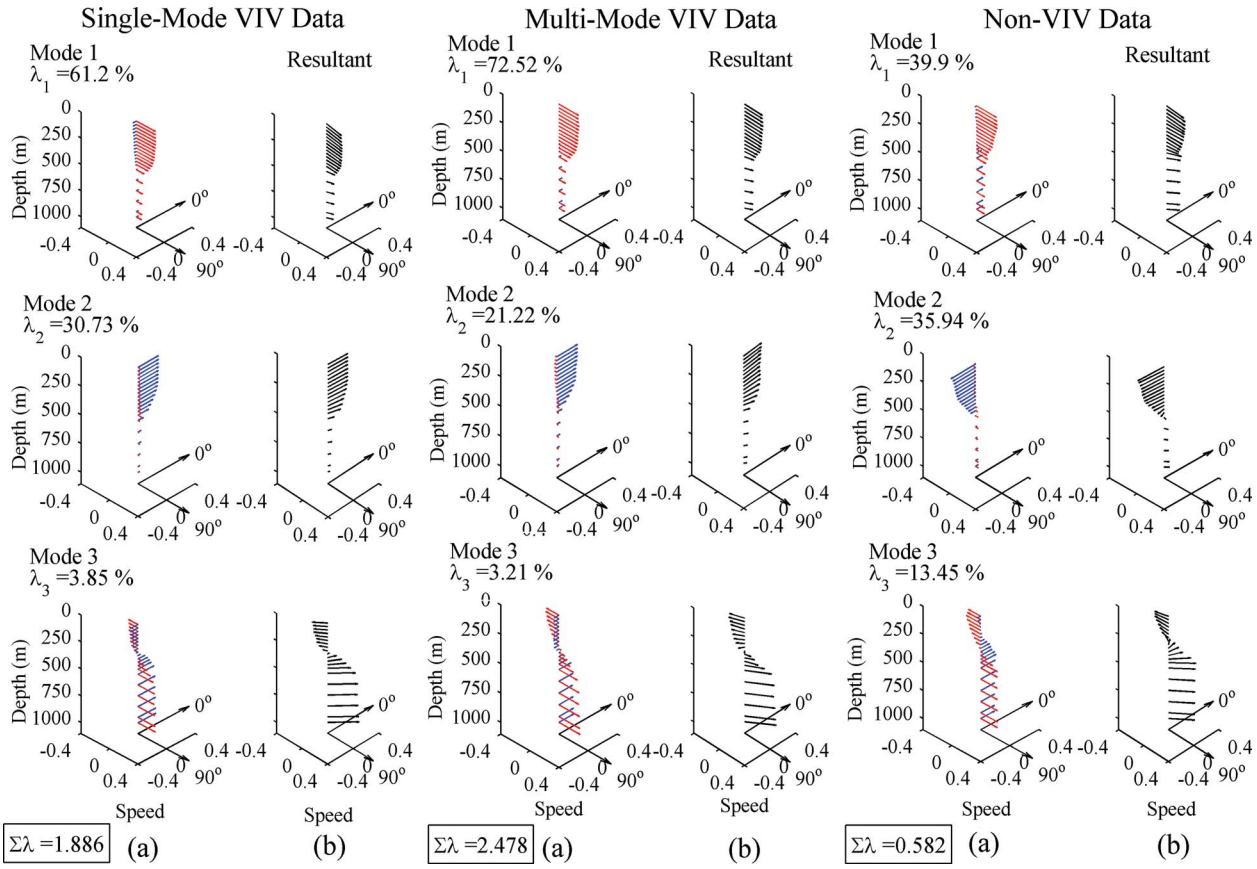

Fig. 11 First three POD mode shapes of current velocity for (*a*) components in the 0 deg and 90 deg directions and (*b*) resultant and associated direction

was conducted. The data were collected over a 2 month period at a deepwater (1000 m) site. POD, a numerical procedure for describing the spatial coherence in a random field, was used to establish dominant energetic current profiles that could be considered in riser design since the traditional approach where current velocities at each depth are treated independently may be overly conservative. The efficiency and accuracy resulting from the use of a limited number of POD modes were studied by comparing measured current velocity profiles with those reconstructed based on a reduced-order truncation. In order to identify and analyze VIV for this riser, in-line and cross-flow motions in different data segments were studied using spectral methods. POD procedures were again employed; this time, to empirically estimate vibration modes participating in the measured riser response data. Finally, the relationship between riser response of different types and coincident current profiles was evaluated with the help of POD techniques that identified patterns in the current profiles that accompanied both VIV and non-VIV response.

Full-scale field data on current velocities and riser motions can prove to be invaluable in studies of VIV response of deepwater risers. Spectral and statistical analysis procedures as presented here can be applied as was shown. Results suggest that empirical techniques such as POD can be useful in deriving energetic current profiles for riser design.

Acknowledgment

The authors acknowledge the assistance of BP in providing the current velocity and riser acceleration data used here.

References

[1] Lumley, J. L., 1970, *Stochastic Tools in Turbulence*, Academic, New York.
[2] Karhunen, K., 1946, "Zur spektraltheorie stochastischer prozesse," Ann. Acad. Sci. Fenn., Ser. A1: Math.-Phys., **34**, pp. 1–7.
[3] Loève, M., 1955, *Probability Theory*, Van Nostrand, Princeton, NJ.
[4] Saranyasoontorn, K., and Manuel, L., 2005, "Low-Dimensional Representations of Inflow Turbulence and Wind Turbine Response Using Proper Orthogonal Decomposition," ASME J. Sol. Energy Eng., **127**(4), pp. 553–562.
[5] Srivilairit, T., 2006, "A Study of Current Velocity Profiles and Vortex-Induced Vibration for Deepwater Drilling Risers," MS thesis, University of Texas at Austin, Austin, TX.
[6] Forristall, G. Z., and Cooper, K. C., 1997, "Design Current Profiles Using Empirical Orthogonal Function (EOF) and Inverse FORM Methods," Offshore Technology Conference, Houston, TX, Paper No. OTC 82672, pp. 11–21.
[7] Jeans, G., and Feld, G., 2001, "A Method for Deriving Extreme Current Profiles to Support Design of Deep Water Drilling Risers," *Proceedings of the 20th International Conference on Offshore Mechanics and Arctic Engineering*, Rio de Janeiro, Brazil, Vol. 1, pp. 499–510.
[8] Meling, T. S., and Eik, K. J., 2002, "An Assessment of EOF Current Scatter Diagrams With Respect to Riser VIV Fatigue Damage," *Proceedings of the 21st International Conference on Offshore Mechanics and Arctic Engineering*, Oslo, Norway, Vol. 1, pp. 85–93.
[9] Kleiven, G., 2002, "Identifying VIV Vibration Modes by Use of the Empirical Orthogonal Functions Technique," *Proceedings of the 21st International Conference on Offshore Mechanics and Arctic Engineering*, Oslo, Norway, Vol. 1, pp. 711–719.
[10] Aschheim, M. A., Black, E. F., and Cuesta, I., 2002, "Theory of Principal Components Analysis and Applications to Multistory Frame Buildings Responding to Seismic Excitation," Eng. Struct., **24**, pp. 1091–1103.
[11] Feeny, B. F., 2002, "On Proper Orthogonal Co-Ordinates as Indicators of Modal Activity," J. Sound Vib., **255**(5), pp. 805–817.
[12] Srivilairit, T., and Manuel, L., 2006, "Identification and Analysis of Vortex-Induced Vibrations of a Drilling Riser Using Empirical and Spectral Procedures," *Proceedings of the 16th International Offshore and Polar Engineering Conference*, San Francisco, CA, pp. 824–827.
[13] Kaasen, K. E., 2000, "Identification of Modes of VIV on a Drilling Riser From Measurements of Acceleration and Rate of Rotation," *Proceedings of the Tenth International Offshore and Polar Engineering Conference*, Seattle, WA, Vol. 2, pp. 23–28.
[14] Isherwood, R. M., 2007, "ORCAFLEX VIV Toolbox Validation: Comparisons With Measured Data from Schiehallion Drilling Riser," Orcina Ltd., Report No. R648-03-02.
[15] Vandiver, J. K., Allen, D., and Li, L., 1996, "The Occurrence of Lock-In Under Highly Sheared Condition," J. Fluids Struct., **10**, pp. 555–561.